Astronomical and Astrophysical Transactions (*AApTr*), 2012, Vol. 27, Issue 3, pp. 447–454,
ISSN 1055-6796, Photocopying permitted by license only, ©Cambridge Scientific Publishers

The spectrum of gas emission in selected regions of the Irr starburst galaxy IC 10

O.V. Egorov[1*], T.A. Lozinskaya[1†], A.V. Moiseev[2]

[1] *Sternberg Astronomical Institute, Lomonosov Moscow State University, 13 Universitetskii Pr., Moscow, 119992 Russia*
[2] *Special Astrophysical Observatory, Russian Academy of Sciences, Nizhnii Arkhyz, Karachai-Cherkessia, Russia*

Received 20 November, 2008

We present the results of observations of the Irr galaxy IC 10 at the SAO RAS 6-m telescope with the SCORPIO focal reducer operating in the long-slit spectrograph mode. The work has been continued after the conference and here we add the new results of the integral-field MPFS observations of the galaxy. Based on these data we have analyzed the ionized-gas emission spectrum in the region of intense star formation and refined the gas metallicity estimates. Using the new improved ionization models by Martin-Manjon et al. [1], we have determined the gas ionization parameters and ionizing-clusters ages and masses from the spectra of the investigated HII regions. The cluster ages and masses are shown to be within the ranges 2.5–5 Myr and $(0.2–1)\times10^5 M_\odot$, respectively. We have determined the relative O/H, N/H and S/H abundances in about twenty HII regions of the galaxy.

Keywords: Galaxies; Star formation; Spectra; IC10

1 Introduction

H_α and [SII] line images of the Irr galaxy IC 10 show a giant complex of multiple shells and supeshells with sizes ranging from 50 to 500–800 pc (see Fig. 1).

The stellar population of the galaxy and anomalously high space density of WR stars are indicative of almost "synchronous" and short burst of ongoing star formation, which, however, must have spread throughout most of the galaxy. It is the place where the currently most confidently identified hypernova remnant – the Synchrotron Supershell – is located [2].

2 Observations

Five spectrograms were taken at the SAO RAS 6-m telescope with SCORPIO focal reducer [3] operating in the long-slit spectrograph mode. We also add here the new

*Email: egorov@sai.msu.ru
†Email: lozinsk36@mail.ru

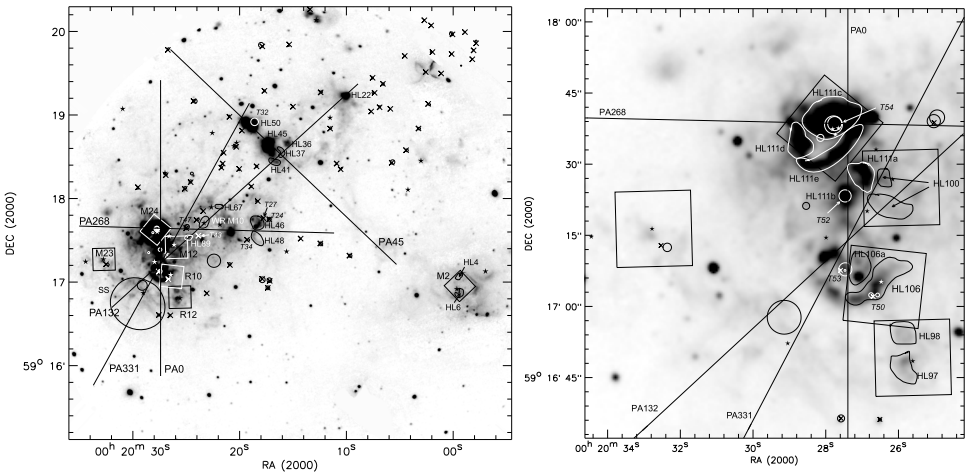


Figure 1 Localization of the long-slit spectrograms and MPFS fields on the H_α image of IC 10: (left) the entire galaxy and (right) the brightest region of current star formation. The asterisks mark the spectroscopically confirmed WR stars, the circles and crosses – stellar clusters. Also shown are the HII regions over which the lines presented in Table 1 were integrated.

results obtained after the conference at the 6-m telescope with the integral-field spectrograph MPFS [4]. Figure 1 shows the locations of the slit spectrograms and MPFS fields on the H_α image of IC10.

The spatial and spectral resolutions were equal to $0.36''$/pixel and about 5 Å respectively along the slit and $1''$/pixel and 6.5 Å for MPFS spectra.

Relative abundance of oxygen is derived from the spectra obtained using the Pettini and Pagel [5] calibration of $12 + \log(\mathrm{O/H})$ as a function of $[\mathrm{NII}]/\mathrm{H}_\alpha$ and $[\mathrm{OIII}]/\mathrm{H}_\beta$ line intensities ratios. We averaged the abundance over HII regions from the catalog of Hodge and Lee [6].

We have defined relative ionic abundance of N^+ and S^+, using a method described in [7]. Using the results of our work [8] we have determined ionization correction factors (ICF) for these ions to take into account unobservable ionization states and estimated total abundance of nitrogen and sulfur by method [7].

The results are summarised in Table 1. Columns 1, 2, 3, 4 and 5 give the name of the region according to [6], the inferred $12+\log(\mathrm{O/H})$, $12+\log(\mathrm{N}^+/\mathrm{H})$, $12+\log(\mathrm{N/H})$, $12 + \log(\mathrm{S}^+/\mathrm{H})$, $12 + \log(\mathrm{S/H})$ values, respectively. The errors here do not include uncertainties of the method (± 0.2 dex). Unfortunately, we have no measurments of the $[\mathrm{SIII}]\lambda 6312$ Å line intensities because of its low signal/noise ratio. Therefore, the value of total sulfur abundance does not include the S^{2+} ion and may be underestimated.

3 Discussion

We reveal strong variations of **interstellar extinction** between different HII regions, which explain the discrepancies between early extinction and distance estimates for

IC 10. The observed variations may be due to "local" extinction in the central star-forming region, which resides in the direction of the densest cloud of neutral and molecular gas and is possibly partially embedded in it. We adopt E(B-V) = 0.95^m [8] in this paper.

Our results provide the currently most detailed **O, N and S relative abundances** for the galaxy. Until recently, abundances were estimated only for the two brightest regions HL111 and HL45 [9, 10]. Our measurements show the oxygen abundance to vary over a wide range for different HII regions in the galaxy. The mean abundance averaged over the regions studied is $12+\log(\mathrm{O/H}) \simeq 8.30\pm0.31$. The mean oxygen abundance in the brightest shell HL111 is equal to $12+\log(\mathrm{O/H}) = 8.17\pm0.24$.

The oxygen abundance variations in the interstellar medium of IC 10, up to several tenths of dex, were considered recently by Magrini and Gonçalves [11], who pointed out the region of the most constant oxygen abundance $12 + \log(\mathrm{O/H}) = 8.2$ at a galactocentric distance of 0.2–0.5 kpc.

Note that for four regions common to our measurements and that by Magrini and Gonçalves [11], the results are in good agreement.

The line intensity ratio of I([SII])/I(H_α)=0.7–1.0 in the **Synchrotron Supershell** (named SS in Table 1) strongly suggests a gas emission behind the shock front. This is also evidenced by the higher I([NII]6548+6584)/I(H_α) $\simeq$ 0.25 and I([OII]3727)/I([OIII]5007) $\simeq$ 1.58 ratios and the lower I([OIII]5007)/I(H_β) $\simeq$ 0.15 ratio than those in the nearby bright HII region HL106. The inferred estimate of oxygen abundance in the Synchrotron Supershell is ambiguous. The models of the gas emission behind the shock front (Allen et al., 2008) allow us to determine the oxygen abundance from the available line intensities if the ambient gas density and the shock velocity are known. However, the problem is complicated by the presence of the WR star M17 in the central region of the synchrotron supershell, whose ionizing radiation may be important for its neighborhoods.

On the other hand, gas emission behind the shock front must be taken into account for the technique used for HII regions to be correctly applicable in our case. We therefore derive provisional oxygen abundance estimates using the two methods while being fully aware of the incorrectness of both approaches.

We found $12 + \log(\mathrm{O/H}) = 8.50 \pm 0.29$ for the Synchrotron Supershell based on the spectrograms interpreted in terms of the HII region model.

Comparison with the models of gas emission behind the front of a shock propagating with the velocity 100 km/s [13] gives the best agreement at an abundance $12 + \log(\mathrm{O/H}) \simeq 8.15$ for the models of purely collisional excitation or $12 + \log(\mathrm{O/H}) \simeq 8.35$ for the models including the gas pre-ionization by a shock.

We have used the theoretical photoionization models from [1] for the metallicity determined above to estimate the masses and ages of ionizing clusters for some of the HII regions. The results are presented in Table 2. Columns 1, 2, 3, 4, 5 and 6 give respectively the name of the region according to [6], the names of ionizing clusters according to [14] (the sign "?" marks the clusters that are probable ionization sources of the corresponding HII region), H_β–luminosities, obtained ages, masses of clusters and ionization parameters. Details of this analysis are published in [15].

We estimated the amount of O5V stars needed to ionize the gas in the HL111 nebula using measured H_β-luminosity and the photon UV-luminosity of O5V star $Q_0 = 1.6 \times 10^{49}$ photons/s for metallicity $Z = 0.2Z\odot$ from [16].

Table 1 Oxygen, nitrogen and sulfur relative abundances.

HII region	$12+\log(\mathrm{O/H})$	$12+\log(\mathrm{N^+/H})$	$12+\log(\mathrm{N/H})$	$12+\log(\mathrm{S^+/H})$	$12+\log(\mathrm{S/H})$
Observations with MPFS					
HL111c	8.16 ± 0.04	6.51 ± 0.10	—	5.91 ± 0.13	—
HL111d	8.17 ± 0.04	6.56 ± 0.11	—	6.02 ± 0.10	—
HL111e	8.23 ± 0.03	6.67 ± 0.08	—	6.16 ± 0.13	—
HL100	8.43 ± 0.04	7.21 ± 0.15	–	6.89 ± 0.17	–
HL111a	8.29 ± 0.05	6.95 ± 0.10	–	6.50 ± 0.12	–
HL106	8.36 ± 0.05	6.81 ± 0.33	–	6.43 ± 0.43	–
HL106a	8.31 ± 0.03	6.61 ± 0.11	–	6.08 ± 0.14	–
HL97	8.26 ± 0.06	6.93 ± 0.28	–	6.54 ± 0.31	–
HL98	8.35 ± 0.05	7.17 ± 0.41	–	6.92 ± 0.42	–
HL4	8.30 ± 0.16	7.28 ± 0.41	–	6.24 ± 0.22	–
HL6	8.18 ± 0.12	7.51 ± 0.22	–	7.02 ± 0.12	–

©2012 Astronomical and Astrophysical Transactions (AApTr), Vol. 27, Issue 3

Table 1 (continued)

HII region	$12 + \log(\mathrm{O/H})$	$12 + \log(\mathrm{N^+/H})$	$12 + \log(\mathrm{N/H})$	$12 + \log(\mathrm{S^+/H})$	$12 + \log(\mathrm{S/H})$
Observations with long-slit spectrograph					
HL111a	8.33 ± 0.04	6.73 ± 0.13	7.00 ± 0.15	6.10 ± 0.03	6.08 ± 0.03
HL111b	8.41 ± 0.01	6.86 ± 0.02	7.03 ± 0.02	6.09 ± 0.01	6.09 ± 0.01
HL111c	8.18 ± 0.01	6.45 ± 0.10	6.93 ± 0.12	5.67 ± 0.09	5.71 ± 0.09
HL111d	8.26 ± 0.01	6.70 ± 0.01	7.05 ± 0.01	5.95 ± 0.01	5.97 ± 0.01
HL111e	8.29 ± 0.01	6.69 ± 0.02	6.98 ± 0.04	5.97 ± 0.01	5.98 ± 0.01
HL106	8.27 ± 0.05	6.65 ± 0.23	6.99 ± 0.23	6.00 ± 0.07	6.01 ± 0.07
SS	8.50 ± 0.09	7.07 ± 0.26	7.27 ± 0.27	6.61 ± 0.10	6.63 ± 0.11
HL37	8.15 ± 0.12	6.71 ± 0.34	7.12 ± 0.34	5.86 ± 0.05	5.87 ± 0.05
HL45	8.08 ± 0.01	6.13 ± 0.10	6.86 ± 0.12	5.74 ± 0.01	5.92 ± 0.05
HL50	8.18 ± 0.08	6.54 ± 0.39	6.95 ± 0.40	5.81 ± 0.34	5.82 ± 0.34
HL100	8.42 ± 0.02	6.90 ± 0.06	7.11 ± 0.06	6.28 ± 0.02	6.28 ± 0.02
HL89	8.44 ± 0.04	6.93 ± 0.03	7.08 ± 0.04	6.29 ± 0.03	6.29 ± 0.03
WR M10	8.42 ± 0.02	7.02 ± 0.07	7.13 ± 0.07	6.45 ± 0.03	6.45 ± 0.03
HL67	8.39 ± 0.04	6.94 ± 0.24	7.09 ± 0.24	6.20 ± 0.07	6.21 ± 0.07
HL41	8.38 ± 0.02	6.95 ± 0.12	7.51 ± 0.22	6.04 ± 0.04	6.11 ± 0.13
HL36	8.20 ± 0.02	6.70 ± 0.14	7.19 ± 0.15	5.72 ± 0.04	5.76 ± 0.05
HL22	8.38 ± 0.01	6.91 ± 0.11	7.13 ± 0.11	5.98 ± 0.03	5.99 ± 0.03
HL46-48	8.45 ± 0.01	7.00 ± 0.09	7.20 ± 0.09	6.27 ± 0.04	6.27 ± 0.04

©2012 Astronomical and Astrophysical Transactions (AApTr), Vol. 27, Issue 3

Table 2 Parameters of the HII regions and the clusters ionizing them.

Region	Cluster	$L(\mathrm{H}\beta)$, 10^{38} erg s^{-1}	Age, Myr	Mass, $10^5 M_\odot$	lg(U)
HL111	T54	3.89	3.5–5.0	1.0–1.5	–2.5
HL106	T50, T53	3.09	4.0–4.5	0.4–1.0	–3.0
HL50	T32	–	3.4–3.6 or 2.5–3.0	1.5–2.0 or 0.4–1.0	–2.47
HL111a,b HL100	T52	–	3.8–4.5	0.2–0.6	–3.27
HL46-48	T34?, T24, T27	–	4.0–5.0	0.2–0.4	–3.6
HL89	T47, T43?	–	>3	≥0.2	–

We found that 10^{51} photons are needed for ionization HL111 nebula, that correspond to about 60 O5V stars.

Acknowledgements

This work is supported by the Russian Foundation for Basic Research (project nos. 07–02–00227 and 10–02–00091) and is based on observational material obtained with the 6-m telescope of the Special Astrophysical Observatory of the Russian Academy of Sciences funded by the Ministry of Science of the Russian Federation (registration number 01-43). Egorov O. V. and Moiseev A. V. are grateful to Dynasty Foundation for financial support.

References

[1] M.L. Martín-Manjón, M.L. García-Vargas, M. Mollá, and A.I. Díaz, MNRAS, **403**, 2012 (2010).
[2] Lozinskaya T.A., Moiseev A.V., MNRAS, **381**, 26L (2007).
[3] Afanasiev V.L., Moiseev A.V., Astron. Lett., **31**, 193 (2005).
[4] Afanasiev V.L., Dodonov S.N., Moiseev A.V., in Ossipkov L.P., Nikiforov I.I., eds, Stellar Dynamics: From Classic to Modern, St Petersburg, p. 103 (2001).
[5] Pettini M., Pagel B.E.J., MNRAS, **348**, 59 (2004).
[6] Hodge P., Lee M.G., PASP, **102**, 26 (1990).
[7] Izotov Y.I., Stasinska G., Meynet G., Guseva N.G., Thuan T.X., Astron. Astrophys., **448**, No. 3, 955-970 (2006).
[8] T.A. Lozinskaya, O.V. Egorov, A.V. Moiseev, and D.V. Bizyaev, Astron. Lett. **35**, 730 (2009).
[9] Lequeux J., Peimbert M., Rayo J.F., Serrano A., Torres-Peimbert S., AAp, **80**, 155 (1979).
[10] Garnett D.R. Astrophys. J., **363**, 142, (1990).
[11] Magrini L., Gonçalves D.R., MNRAS, **398**, 280 (2009).

[12] Allen M.G., Grovs B.A., Dopita M.A., Sutherland R.S., Kewley L.J., ApJ Suppl. Ser., **178**, 20 (2008).
[13] Lozinskaya T.A., Moiseev A.V., Podorvanyuk N.Yu., Burenkov A.N., Astron. Lett. **34**, 217 (2008).
[14] N. A. Tikhonov, O. A. Galazutdinova, Astron. Lett. **35**, 748 (2009).
[15] Arkhipova V.P., Egorov O.V., Lozinskaya T.A., Moiseev A.V., Astron. Lett., **37**, 65 (2011).
[16] Smith L. J. et al., MNRAS, **337**, 1309-1328 (2002).